EUROPEAN ORGANIZATION FOR NUCLEAR RESEARCH

CERN-EP/90-15
29 January 1990

A STUDY OF THE POINT-LIKE INTERACTIONS OF THE PHOTON USING ENERGY-FLOWS IN PHOTO- AND HADRO- PRODUCTION FOR INCIDENT ENERGIES BETWEEN 65 AND 170 GeV

The OMEGA Photon Collaboration

R. J. APSIMON[5], M. ATKINSON[3], M. BAAKE[1], L. S. BAGDASARIAN[7], D. BARBERIS[2], T. J. BRODBECK[4], N. BROOK[3], T. CHARITY[4], A. B. CLEGG[4], P. COYLE[3], S. DANAHER[6], S. DANAGULIAN[7], M. DAVENPORT[2], B. DICKINSON[3], B. DIEKMANN[1], A. DONNACHIE[3], A. T. DOYLE[3], J. EADES[2], R. J. ELLISON[3], P. S. FLOWER[5], J. M. FOSTER[3], W. GALBRAITH[6], P. I. GALUMIAN[7], C. GAPP[1], F. GEBERT[1], G. HALLEWELL[5], K. HEINLOTH[1], R. C. W. HENDERSON[4], M. T. HICKMAN[4], C. HOEGER[1], A. HOLZKAMP[1], S. HOLZKAMP[1], R. E. HUGHES-JONES[3], M. IBBOTSON[3], H. P. JAKOB[1], D. JOSEPH[1], N. R. KEEMER[4], J. KINGLER[1], G. KOERSGEN[1], S. D. KOLYA[3], G. D. LAFFERTY[3], H. M^{C}CANN[3], R. M^{C}CLATCHEY[2], C. M^{C}MANUS[3], D. MERCER[3], J. A. G. MORRIS[5], J. V. MORRIS[5], D. NEWTON[4], A. O'CONNOR[4], R. OEDINGEN[1], A. G. OGANESIAN[7], P. J. OTTEWELL[3], C. N. PATERSON[5], E. PAUL[1], D. REID[3], H. ROTSCHEIDT[1], P. H. SHARP[5], S. SOELDNER-REMBOLD[1], N. A. THACKER[6], L. THOMPSON[6], R. J. THOMPSON[3], J. WATERHOUSE[3], A. S. WEIGEND[1], G. W. WILSON[4].

Bonn [1] - *CERN* [2] - *Manchester* [3] - *Lancaster* [4] - *RAL* [5] - *Sheffield* [6] - *Yerevan* [7].

ABSTRACT

Energy-flow distributions for charged hadrons from interactions of photons, pions and kaons on hydrogen are presented as functions of $\sum p_T^2$ in the event plane. Data cover the range $0.0 < \sum p_{T\,in}^{2} < 10.0$ (GeV/c)^2 and $0.0 < x_F < 1.0$ for beam momenta from 65 to 170 GeV/c. The comparisons between photon- and hadron-induced data show an excess of events with larger $\sum p_{T\,in}^{2}$ for the photon-induced data. Using the hadron-induced data to parameterise the hadronic behaviour of the photon, the differences between cross sections are used to measure the contribution of the point-like photon interactions. Quantitative calculations of the point-like photon interactions using the Lund Monte-Carlo program LUCIFER, based on QCD, are in agreement with the data.

Submitted to Zeitschrift für Physik C

Section 1: Introduction.

Hadronic interactions of the photon arise through a component described by the Vector Meson Dominance (VMD) model, and a component from direct coupling with a parton in the target. The hard nature of the direct component means that it is significant only if the events contain large transverse momenta. At sufficiently large transverse momenta the two components give rise to different topologies; in the case of VMD type processes, the expectation is for the usual 4-jet structure, as opposed to the unique 3-jet structure expected from the direct point-like processes [1]. Higher-twist processes are also expected to be present in small numbers, giving events with similar topologies to the point-like processes. At the energy of this experiment ($\sqrt{s}$ of 11 to 18 GeV) the jets are expected to appear as rather broad overlapping clusters of particles.

The analysis presented here determines the energy-flows in high-p_T events and complements previous work on single-particle inclusive cross sections [2,3]. Photon- and hadron-induced data were taken with the OMEGA Spectrometer at CERN. The hadron-like component of the photon was parameterised (assuming the VMD model) by the hadron-induced data taken in the same apparatus. This component could then be subtracted from the photon-induced data, allowing features due to the direct coupling to be seen with minimal biases due to the acceptance of the apparatus.

The experimental data sample and its reduction are discussed in section 2, the topological analysis of the events in section 3 and the normalisation and p_T-dependence in section 4. The energy-flow results are presented in section 5 and compared with a Monte-Carlo simulation in section 6. There is a brief summary in section 7.

Section 2: The data and its reduction.

The data reported in this paper were taken by the WA69 collaboration using the CERN SPS and the OMEGA spectrometer. The total number of photon-induced triggers was $\approx 1.5\ 10^7$ over the momentum range $65 < p_\gamma < 170$ GeV/c. Data were also taken with both pion and kaon beams, of both polarities. The kaon beam was used as a source of valence s and $\bar{s}$ quarks in order to be able to approximate the strange-quark component of the photon. A total of $\approx 2\ 10^7$ hadron-induced triggers was divided between both charges and beam momenta of 80 and 140 GeV/c. The data were taken with a liquid hydrogen target and an open trigger was used to give a largely unbiased sample of events. In this analysis the photon-induced data from 65 to 95 GeV/c and 110 to 170 GeV/c were compared with the 80 GeV/c and 140 GeV/c hadron-induced data respectively. The initial data samples were the same as those used in a recent study of inclusive single charged particles [3] and experimental details have been reported in that paper.

The OMEGA measurements were analysed with a modified version of the program TRIDENT [4] to find and fit tracks and determine the event vertices. All events were discarded which did not belong to the main trigger. Events were only accepted if the reconstructed interaction vertex was inside the hydrogen target and had a minimum of three tracks associated with it. Residual electromagnetic interactions were removed by

eliminating events where all tracks were within a dip of ± 2.5 mrad relative to a plane orthogonal to the OMEGA magnetic field direction.

In the present analysis it was important that only genuine and well-measured individual tracks were included. Contamination of events with badly measured tracks was found to be negligible except for events containing individual tracks with $p_T > 2.0$ GeV/c where errors in determining the track parameters and pattern recognition failures caused some contamination. This is exactly the same situation found in recent studies on single inclusive high-p_T charged particles [3] and hence similar cuts have been used for these high-p_T tracks. The effects of the cuts have been studied using the Lund Monte-Carlo program LUCIFER [5] (see section 6) to generate the basic event and JETSET 6.2 [6] to handle the string fragmentation. These events were used as input to a full detector simulation and the standard analysis chain. The acceptance for individual tracks (discussed in section 6) was found to be uniform at 0.85. The quality of the final selection is demonstrated in later sections.

Section 3: Analysis of the Event Plane.

At the energies of this experiment it is expected that soft physics will lead to a forward peak in the particle distributions. QCD Compton and QCD Bethe-Heitler (see figure 1) processes should lead to two broad clusters in the forward direction. It is not expected that the clusters will be well separated on an event-by-event basis. Hence energy-flows in the event plane were used to isolate topological features on a statistical basis [7,8].

The transverse momentum, $\vec{p_T}$, of each particle can be considered in terms of two components, $p_{T\ out}$ and $p_{T\ in}$, normal and parallel to a particular plane. This plane is the best estimate of the event plane if it is oriented so that the sum of the squares of the momentum components of the produced particles transverse to the plane, $\sum p_{T\ out}^{\ 2}$, is minimized. It then follows that $\sum p_{T\ in}^{\ 2}$ is maximized. If two clusters are present in the forward hemisphere then $\sum p_{T\ in}^{\ 2}$ is expected to develop a tail at higher values. On the other hand $\sum p_{T\ out}^{\ 2}$ should not be sensitive to the presence of two clusters and should reflect only the intrinsic p_T properties of the partons.

The acceptance of the apparatus for π^0-mesons was lower than that for charged particles and was more susceptible to biases. Clearly the event plane found when neutral particles were omitted was in general different from that when they were included. The change in the orientation of the event plane when all detected neutral particles were included has been studied by using LUCIFER events and was found to be typically only $\pm 2.5°$; this was of the same order as the uncertainty introduced by measurement errors on charged tracks. For charged particles the acceptance was virtually constant, independent of p_T, for all $x_F > 0.0$ but fell rapidly elsewhere. Hence for the remainder of the analysis reported here only forward charged particles were used for both the data and the simulation.

The analysis was carried out in the beam-proton c. m. frame. The absence of particles with negative x_F and of neutral particles resulted in the remaining 'event'

being unbalanced in momentum in this frame. A standard sphericity analysis was thus not possible. The true sphericity axis is known to be very close to the beam direction [7] and so the sphericity axis was defined to be along the beam, and all transverse momenta were measured relative to it. Two alternative methods for finding the event plane have been used.

(1) The observed particles' momentum vectors were projected onto the plane normal to the beam axis and a sphericity analysis was performed in this plane by finding the eigenvectors of the momentum tensor. This procedure requires p_T to be balanced, so a missing-p_T vector was added to each event.

(2) The problem of the lack of p_T-balance was bypassed by rotating to examine possible event planes and selecting that which minimized the $\sum p_T{}^2_{out}$ of the observed particles.

Results obtained by the different methods can, in principle, be different so both must be individually compared with simulated data analysed in the same way. In fact all conclusions were found to be indistinguishable, and those from the second method are shown.

Following the above analysis the consequences of the cuts discussed in section 2 can be demonstrated. In figure 2 the actual Monte-Carlo simulated value of $\sum p_T{}^2_{in}$ is shown plotted against the reconstructed value for the same event. The correlation is good and improves with increasing $\sum p_T{}^2_{in}$.

Section 4: Combining and Normalising the Data from Different Beams.

The absolute normalisation of the data was achieved using direct counting of beam-line photons or charged particles throughout the data taking periods. A key element in the experiment was the use of the same detector set-up, the same trigger and the same software for both the photon-beam and hadron-beam data.

The data for each hadron beam type (π^+,π^-, K^+ and K^-) were normalised to unity and the opposite charges added for each particle type. The π and K data were then combined by taking $\frac{2}{3}\pi$ and $\frac{1}{3}$K data so as to approximate the photon's quark content. This hadron data sample was then scaled so that the cross-section matched that of the photon data in the range $1.0 < \sum p_T^2 < 2.0$ (GeV/c)^2 (see figure 3). The region over which the data were normalised was chosen to exclude very low p_T, where trigger acceptance and leading particles can have effects, and high p_T, where the photon data are expected to have the additional contribution above that of VMD. (This procedure was the same as that used in ref [3].) The systematic error in this relative normalisation has been estimated to be $\pm 3\%$ from the freedom of choice in the normalisation range. These data are shown on figure 3(a) and (b) for the two momentum-ranges $65 < p_\gamma < 95$ GeV/c (compared with $p_h = 80$ GeV/c) and $110 < p_\gamma < 170$ GeV/c (compared with $p_h = 140$ GeV/c). The factors by which the observed hadron cross-sections have been scaled down are 169 and 174 for the 80 and 140 GeV/c data respectively. There were $\pm 15\%$ systematic errors on the absolute cross-

sections found in the experiment so the scaling factors correspond to a VMD factor of 172±30 [3,9] for the event topologies selected.

Section 5: Results.

A study was made of the flow of energy in the event plane to search for evidence of forward clusters. The normalised energy for each track was $2E_i/\sqrt{s}$ where E_i is the energy of the ith detected particle and$\sqrt{s}$ is defined for each event by the beam particle 4-momentum. Each track was entered in an energy-flow plot at θ_i with a weight of the normalised energy. θ_i is the angle between the beam direction and the projection of the ith particle's momentum vector onto the event plane. The plot was finally converted to a cross section by using the total measured luminosity. The energy-flows before subtraction are shown on figure 4 for the high energy data in bins of $\sum p_T^2{}_{in}$. The form of the low energy data (not shown) is similar.

The acceptance across the energy-flow plots was studied by using the full detector simulation as discussed in section 2. Figure 5 shows the acceptance for energy-flows above $\sum p_T^2{}_{in} = 2.0$ (GeV/c)^2. The acceptance is the same at all angles.

The scaled hadron data were subtracted from the photon data to give the contribution from the point-like interactions of the photon. The subtracted data are shown on figures 6 and 7 for the two energy ranges considered and for a series of ranges of $\sum p_T^2{}_{in}$. Only data above $\sum p_T^2{}_{in} = 3.0$ (GeV/c)^2 are shown since below this the contributions from the hard processes are small relative to the systematic errors resulting from the relative normalisation uncertainty of the hadron data before the subtraction. At large $\sum p_T^2{}_{in}$ this systematic effect was small and the errors are dominated by the statistics of the photon-induced data.

The selection of high-$\sum p_T^2$ events has a kinematic effect on the energy-flow plots, increasingly depleting the small angle region as $\sum p_T^2$ increases. Differences between the shapes of the energy-flow plots for photon- and hadron-induced processes must be studied to provide information on clusters. Subtracted energy-flow plots, which separate out the contribution due to the point-like interactions, should have a different shape from the corresponding plots for the hadron-induced data. This difference is seen on figure 4 which shows that the additional component from photons is almost exclusively at intermediate angles.

Energy-flows on the two sides of the beam axis have also been calculated separately. These are shown on figure 8 for high energies and high $\sum p_T^2{}_{in}$. Tracks from the cluster which had the greater (lower) total energy have been entered at positive (negative) angles. This distribution explores the sharing of energy between the two clusters and thus gives some additional information.

Section 6: Comparison with Theory.

The Lund Monte-Carlo programs LUCIFER and JETSET 6.2 were used in order to compare the topological features seen in the event plane after the photon-hadron

subtraction with those features expected from theory.

LUCIFER takes into account the QCD Bethe-Heitler, Compton and higher-twist diagrams. The corresponding cross sections at the parton level are calculated to first order of α_s. Since the value of α_s is somewhat arbitrary in lowest order calculations and depends on the chosen Q^2 scale (here defined at the γ/parton level) and the value of Λ_{QCD}, the overall normalization is uncertain. A further smaller uncertainty is due to the freedom in choosing structure functions. Overall there is an uncertainty in the predicted absolute cross-sections of about 60%. The previous study of single-particle p_T distributions [3] gave good agreement between the subtracted data on one hand and LUCIFER and the higher order calculation of Aurenche et. al. [1] on the other. For that analysis LUCIFER was run with its standard parameters and the structure functions of Eichten et.al. [10]. The same set of parameters has been used for this analysis.

The result of the LUCIFER simulation is shown as the histograms on figures 6 and 7. The agreement is good, particularly for higher values of $\sum p_T{}^2_{in}$ where the QCD calculation is expected to be reliable. The measured contribution from the point-like photon at small angles in the event plane is, if anything, below the LUCIFER predictions using string fragmentation. The results of the LUCIFER simulation are also shown on figure 8 and the predictions again agree well with the data. The results of this analysis extend and complement the previously published analysis of single particle production [3].

Section 7: Conclusions.

It has been shown unambiguously that at $\sum p_T{}^2_{in} > 3$ (GeV/c)^2, the charged-particle inclusive energy-flows from photon-beam interactions differ significantly from those with hadron beams. The extra contribution from photons has been shown to agree well with the predictions of QCD Compton, Bethe-Heitler, and higher-twist processes as given by the LUCIFER Monte-Carlo program.

ACKNOWLEDGEMENTS.

We are very grateful to G. Ingelman who did extensive work on LUCIFER and made our theoretical comparison possible.

BMFT -Foerderkennzeichen 05-4BN14P(0) (Fed. Rep. Germany) and SERC (U.K.) helped financially and we acknowledge this. All our technicians, the CERN OMEGA and beam line groups made vital contributions and to them and CERN generally we are indebted for the success of our work.

The computer centres RHRZ at Bonn, RAL, and CERN have been most generous in their support and we are most grateful to them.

REFERENCES.

[1] P. Aurenche et al.: Nucl. Phys. B286 (1987) 553-591, and references contained therein

[2] E. Auge et al.: Phys. Lett. 168B (1986) 163; and
R. Barate et al.: Phys. Lett. 174B (1986) 458

[3] R. J. Apsimon et al.: Z. Phys. C 43 (1989) 63

[4] J. C. Lassalle et al.: CERN-DD/EE/79-2, and NIM 176 (1980) 371-379

[5] G. Ingelman and A. Weigend: DESY report 87-018 (1987), and
CERN pool program W5047 Long write-up (1986)

[6] T. Sjöstrand: Lund preprint LU/TP/85-10 and
CERN pool program W5035 Long write-up (1986)

[7] M. Atkinson et al.: Z. Phys. C26 (1984) 19

[8] M. Arneodo et al.: Z. Phys. C36 (1987) 527,
M. Barth et al.: Nucl. Phys. B192 (1981) 289, and
R. Göttgens et al.: Nucl. Phys. B206 (1982) 349

[9] M. Atkinson et al.: Nucl. Phys. B245 (1984) 189, and references contained therein

[10] E. Eichten at al.: Rev. Mod. Phys 56 (1984) 579

FIGURE CAPTIONS.

Fig 1 The QCD Compton (a) and QCD Bethe-Heitler (b) processes.

Fig 2 The correlation between the reconstructed and generated values of $\sum p_T{}^2_{in}$ using LUCIFER as the generator.

Fig 3 The $\sum p_T{}^2_{in}$ cross-sections for photon data (▪) and hadron data (○), normalised as discussed in section 4. In addition the subtracted cross-section shown (△) gives a measure of the point-like component. The shifts in the subtracted data produced by a ±3% change in the relative normalisation of the hadron data are shown, where significant, by horizontal lines. The results of the LUCIFER simulation are shown as a histogram.

Fig 4 The energy-flow distributions for the photon-induced (▪) and hadron-induced events (○) from the high incident-energy data for a range of values of $\sum p_T{}^2_{in}$ from 0 to 10 $(GeV/c)^2$.

Fig 5 The ratio of the reconstructed to generated energy-flow (i.e. output energy-flow histogram after TRIDENT and event analysis, divided by the corresponding input histogram for simulated data).

Fig 6 The subtracted energy-flow data (△) for the low incident energies. The plots are for the different ranges of $\sum p_T{}^2_{in}$ shown. The shifts in the subtracted data produced by a ±3% change in the relative normalisation of the hadron data are

shown, where significant, by horizontal lines. The predictions of LUCIFER are shown as histograms.

Fig 7 The energy-flow distributions as in Fig 6 but for the high incident-energy data and simulation. The symbols are the same as on Fig 6.

Fig 8 The subtracted energy-flows of the high energy data with the two sides of the beam axis treated separately. The tracks on the side with the larger value of the total energy are plotted at positive θ and those on the side with lower total energy are plotted at negative θ. The LUCIFER simulation is shown as a histogram. The data is shown for $7.0 < \sum p_T^2{}_{in} < 10.0$ (GeV)^2.

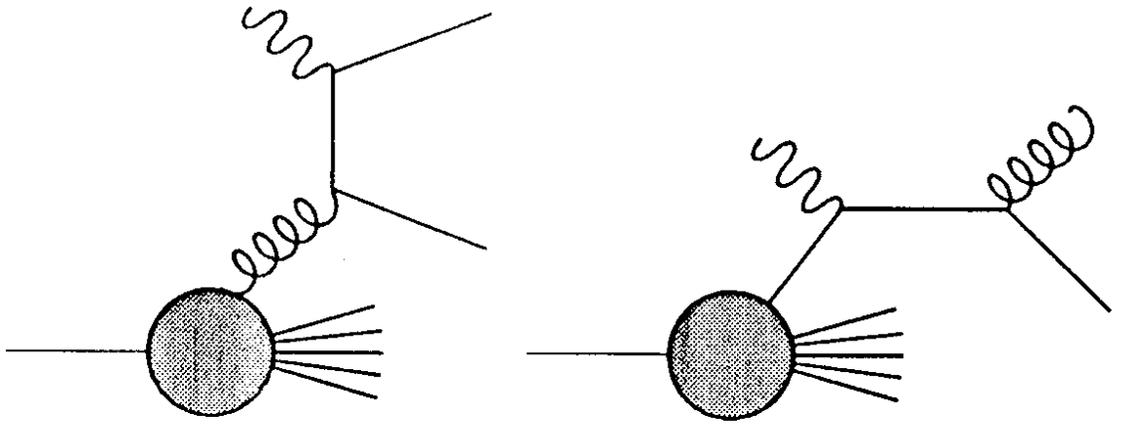

a. b.

Fig. 1

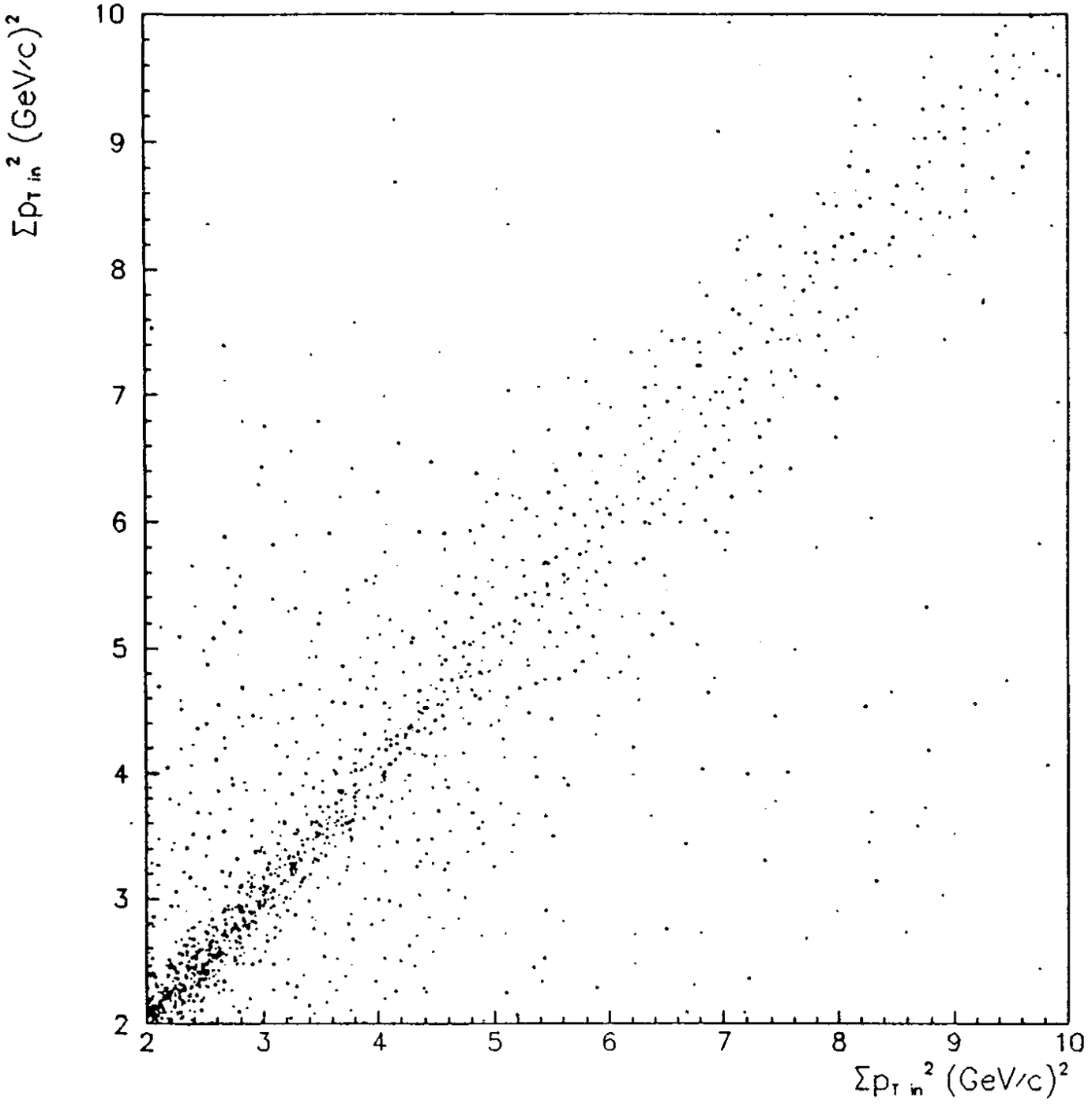

Fig. 2

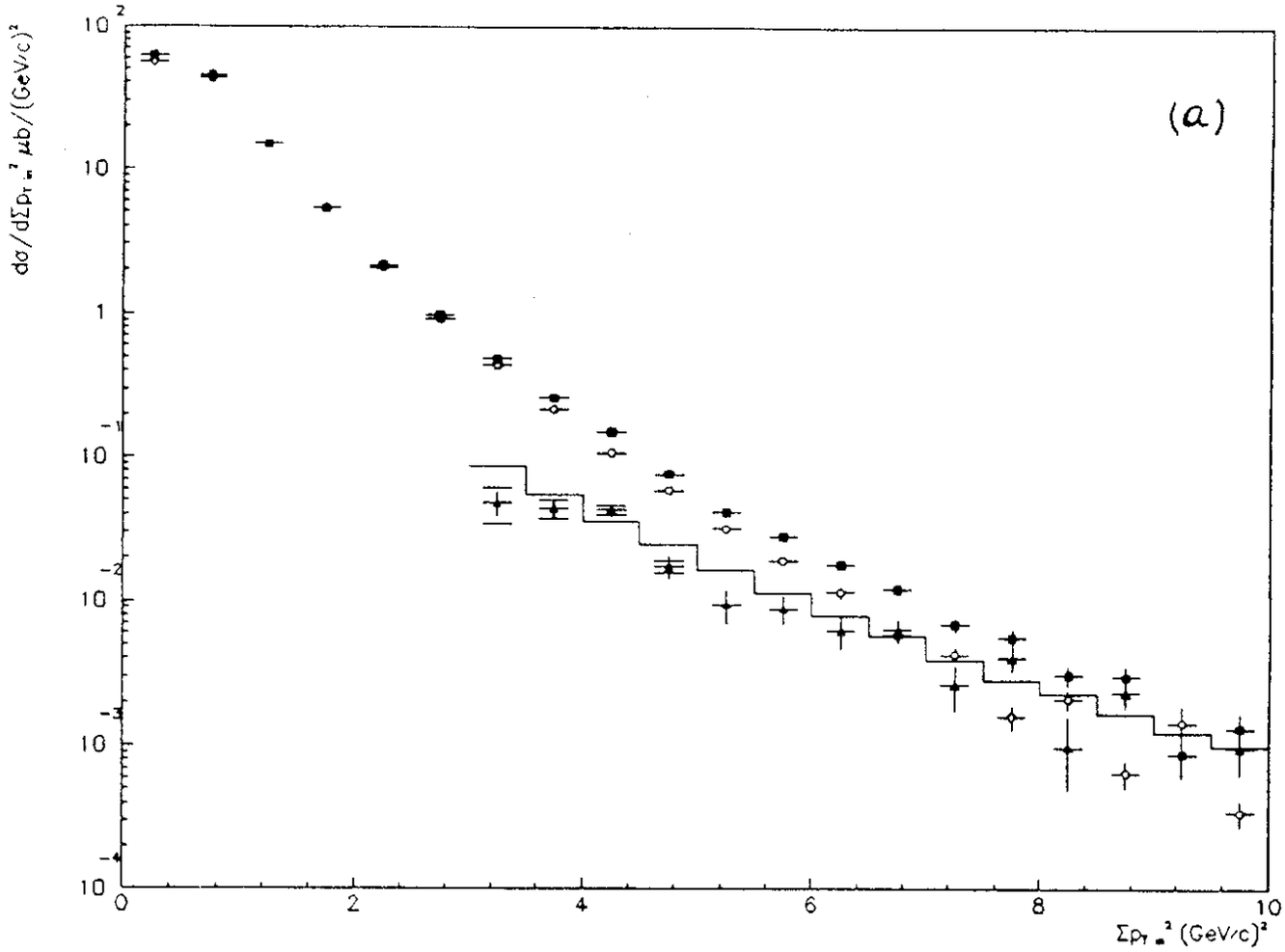
(a)
$d\sigma/d\Sigma p_{T,\pi}{}^2$ μb/(GeV/c)^2
$\Sigma p_{T,\pi}{}^2$ (GeV/c)^2

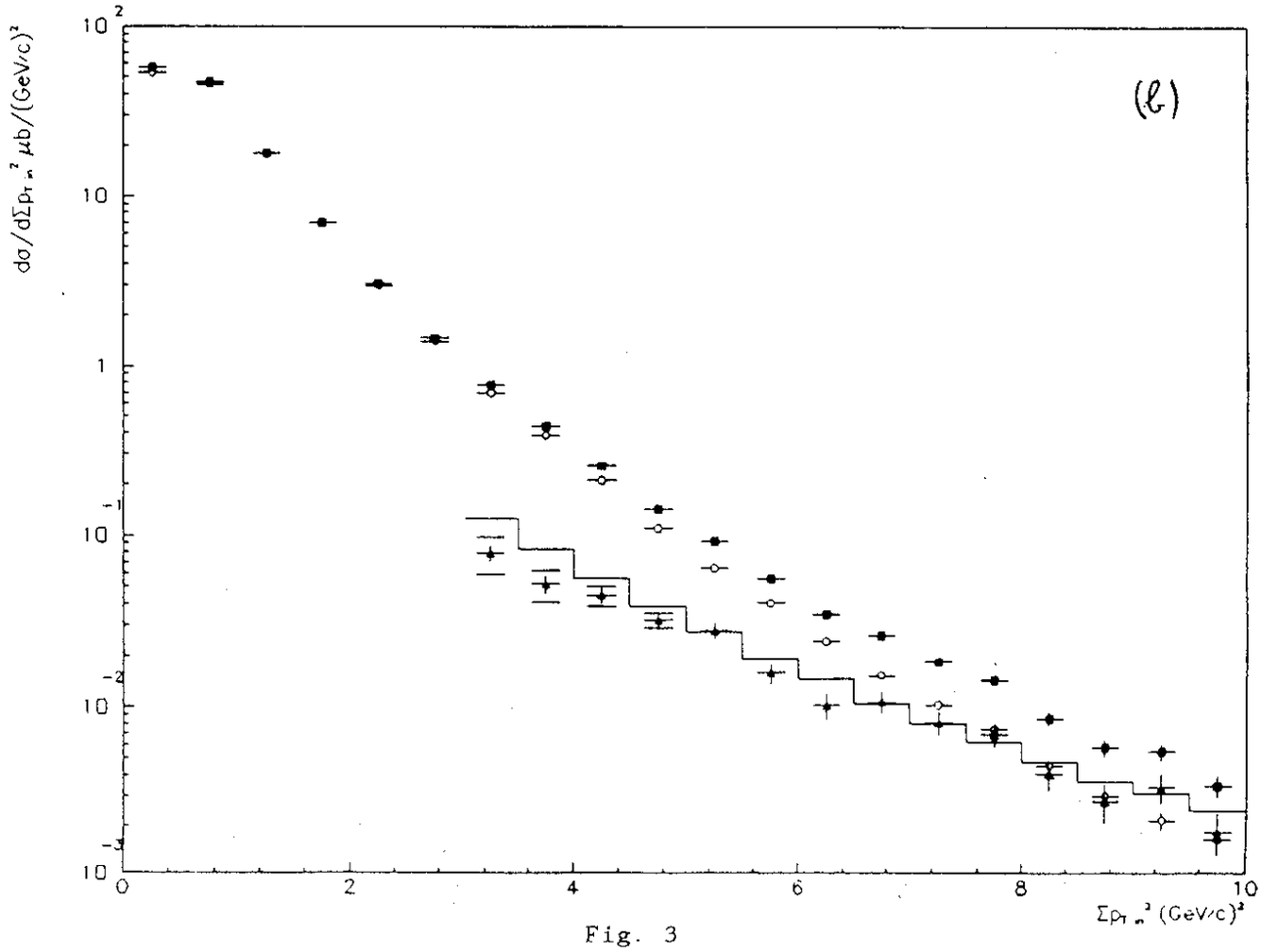
(b)
$d\sigma/d\Sigma p_{T,\pi}{}^2$ μb/(GeV/c)^2
$\Sigma p_{T,\pi}{}^2$ (GeV/c)^2

Fig. 3

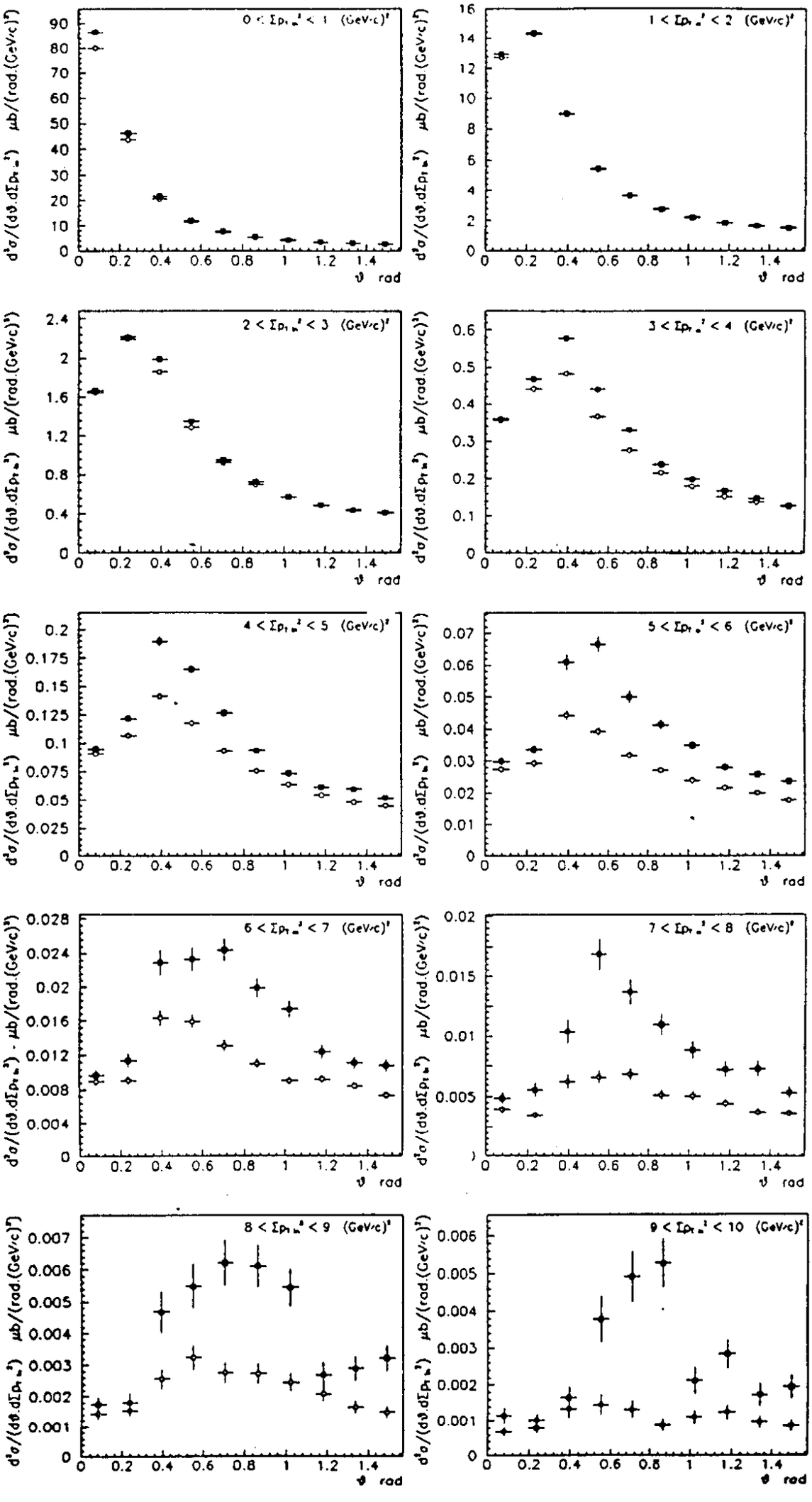
0 < Σp_t,π² < 1 (GeV/c)²
1 < Σp_t,π² < 2 (GeV/c)²
2 < Σp_t,π² < 3 (GeV/c)²
3 < Σp_t,π² < 4 (GeV/c)²
4 < Σp_t,π² < 5 (GeV/c)²
5 < Σp_t,π² < 6 (GeV/c)²
6 < Σp_t,π² < 7 (GeV/c)²
7 < Σp_t,π² < 8 (GeV/c)²
8 < Σp_t,π² < 9 (GeV/c)²
9 < Σp_t,π² < 10 (GeV/c)²
d²σ/(dϑ.dΣp_t,π²) μb/(rad.(GeV/c)²)
ϑ rad

Fig. 4

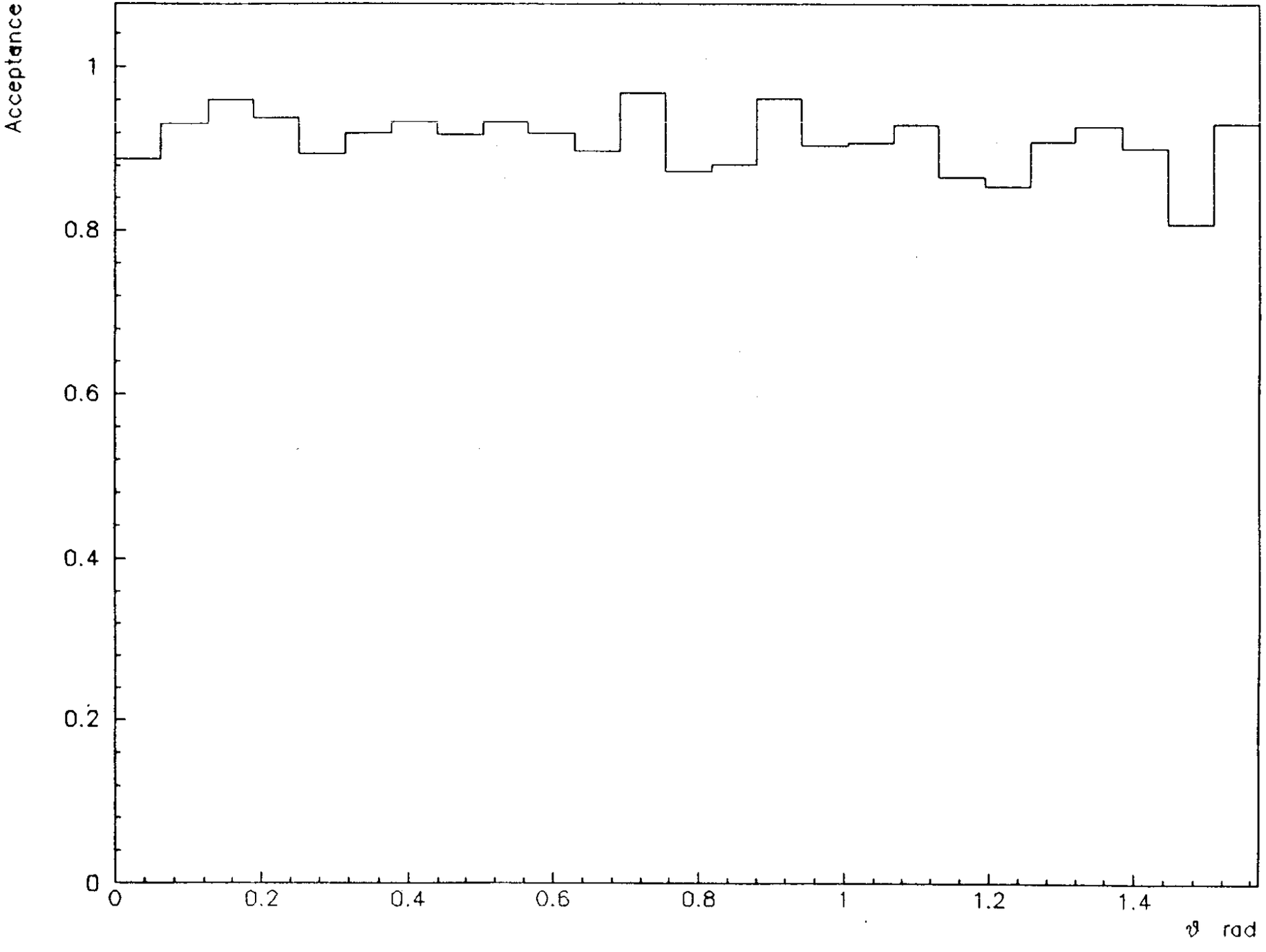

Fig. 5

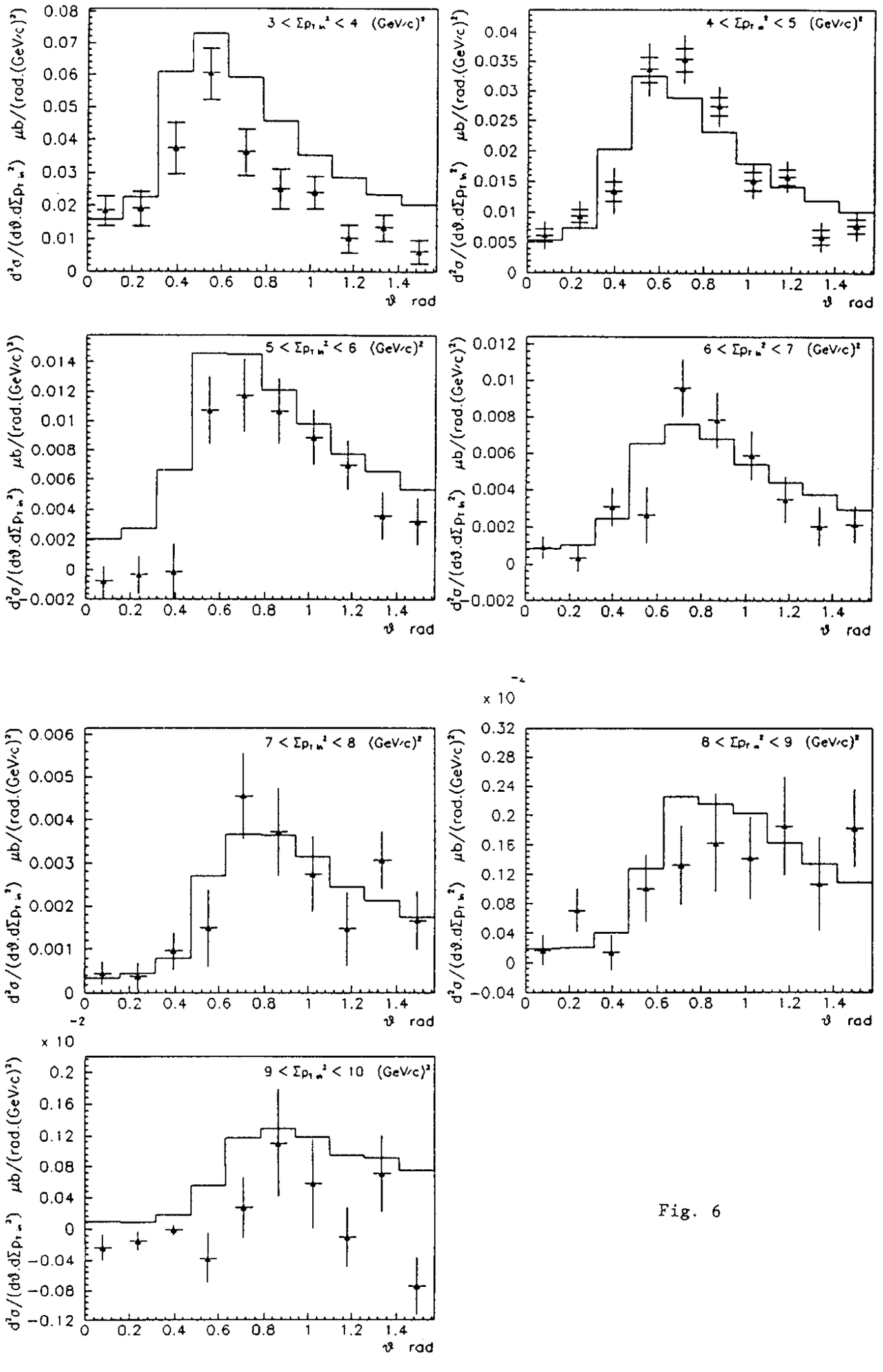
3 < Σp_T,h² < 4 (GeV/c)²
4 < Σp_T,h² < 5 (GeV/c)²
5 < Σp_T,h² < 6 (GeV/c)²
6 < Σp_T,h² < 7 (GeV/c)²
7 < Σp_T,h² < 8 (GeV/c)²
8 < Σp_T,h² < 9 (GeV/c)²
9 < Σp_T,h² < 10 (GeV/c)²
d²σ/(dϑ.dΣp_T,h²) μb/(rad.(GeV/c)²)
ϑ rad
x 10^-2
x 10^-4

Fig. 6

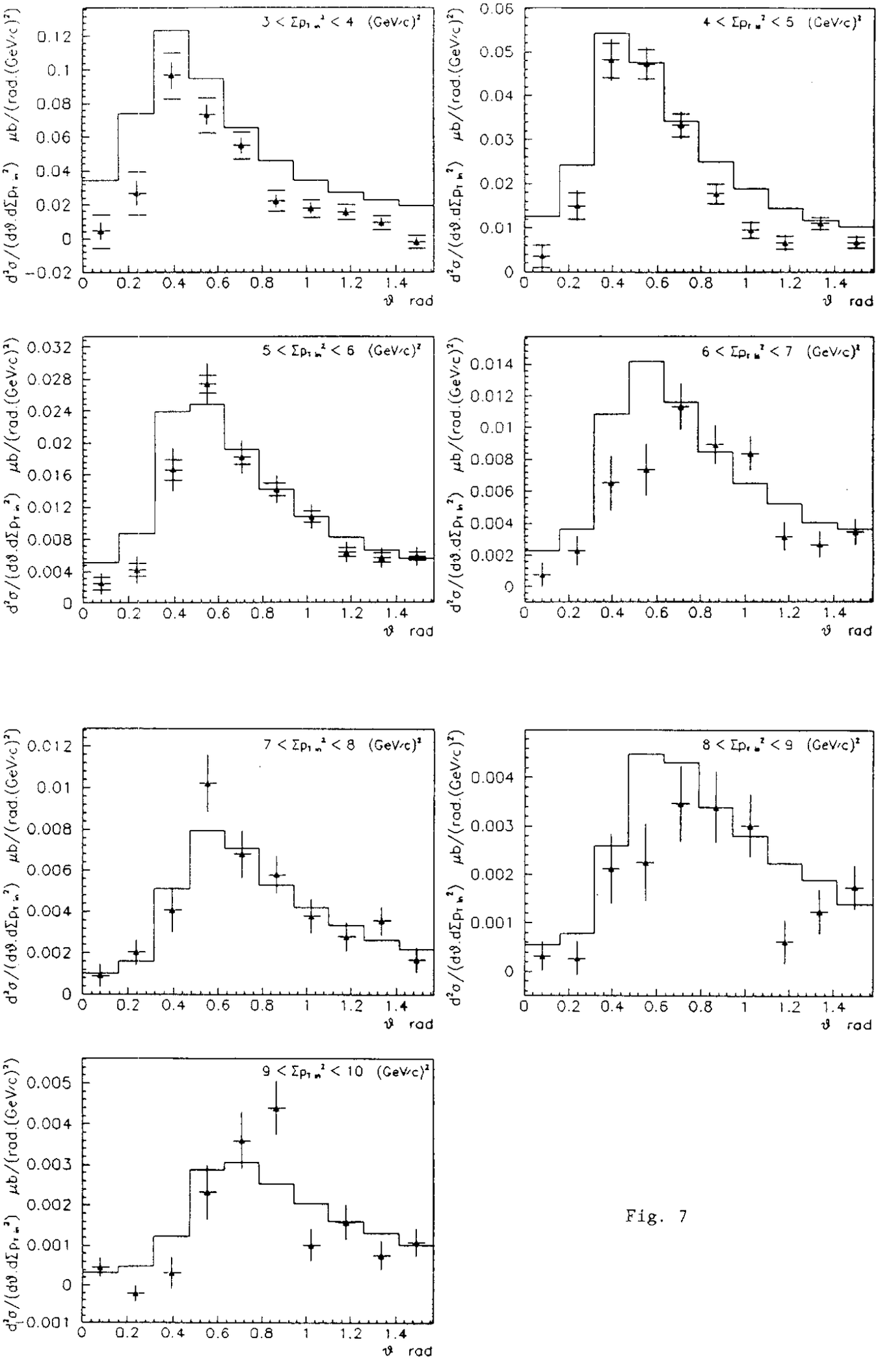
3 < Σp_T,π² < 4 (GeV/c)²
4 < Σp_T,π² < 5 (GeV/c)²
5 < Σp_T,π² < 6 (GeV/c)²
6 < Σp_T,π² < 7 (GeV/c)²
7 < Σp_T,π² < 8 (GeV/c)²
8 < Σp_T,π² < 9 (GeV/c)²
9 < Σp_T,π² < 10 (GeV/c)²
d²σ/(dϑ.dΣp_T,π²) μb/(rad.(GeV/c)²)
ϑ rad

Fig. 7

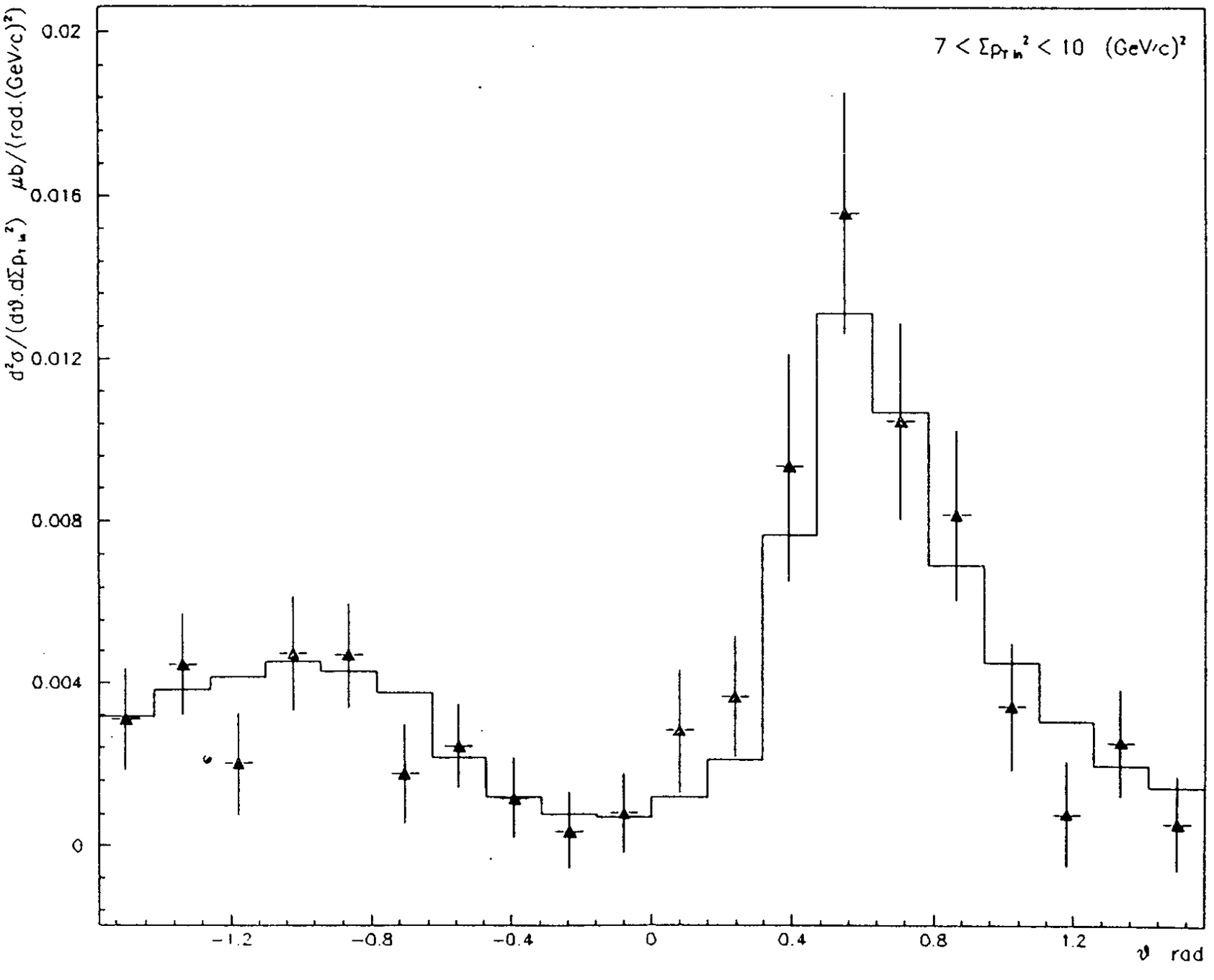
$7 < \Sigma p_{T\,h}^2 < 10$ (GeV/c)²
$d^2\sigma/(d\vartheta.d\Sigma p_{T\,h}^2)$ μb/(rad.(GeV/c)²)
0.02
0.016
0.012
0.008
0.004
0
−1.2
−0.8
−0.4
0
0.4
0.8
1.2
ϑ rad

Fig. 8